Video Article

A Micro-CT-based Method for Characterizing Lesions and Locating Electrodes in Small Animal Brains

Javier Masis[1,2], David Mankus[2], Steffen B.E. Wolff[2,3], Grigori Guitchounts[1,2], Maximilian Joesch[4], David D. Cox[1,2]

[1]Department of Molecular and Cellular Biology, Harvard University

[2]Center for Brain Science, Harvard University

[3]Department of Organismic and Evolutionary Biology, Harvard University

[4]Institute of Science and Technology Austria

Correspondence to: Javier Masis at jmasis@fas.harvard.edu

URL: https://www.jove.com/video/58585
DOI: doi:10.3791/58585

Keywords: Neuroscience, Issue 141, micro-CT, lesion, electrode, neuroscience, rat, rodent, zebra finch

Date Published: 11/8/2018

Citation: Masis, J., Mankus, D., Wolff, S.B., Guitchounts, G., Joesch, M., Cox, D.D. A Micro-CT-based Method for Characterizing Lesions and Locating Electrodes in Small Animal Brains. *J. Vis. Exp.* (141), e58585, doi:10.3791/58585 (2018).

Abstract

Lesion and electrode location verification are traditionally done *via* histological examination of stained brain slices, a time-consuming procedure that requires manual estimation. Here, we describe a simple, straightforward method for quantifying lesions and locating electrodes in the brain that is less laborious and yields more detailed results. Whole brains are stained with osmium tetroxide, embedded in resin, and imaged with a micro-CT scanner. The scans result in 3D digital volumes of the brains with resolutions and virtual section thicknesses dependent on the sample size (12–15 and 5–6 µm per voxel for rat and zebra finch brains, respectively). Surface and deep lesions can be characterized, and single tetrodes, tetrode arrays, electrolytic lesions, and silicon probes can also be localized. Free and proprietary software allows experimenters to examine the sample volume from any plane and segment the volume manually or automatically. Because this method generates whole brain volume, lesions and electrodes can be quantified to a much higher degree than in current methods, which will help standardize comparisons within and across studies.

Video Link

The video component of this article can be found at https://www.jove.com/video/58585/

Introduction

Neuroscientists have relied on lesions for a long time in order to understand the relationship between function and location in the brain. For example, our understanding of the hippocampus as being indispensable for learning and memory and of the prefrontal cortex as being key for impulse control were both products of serendipitous lesions in humans[1,2]. The use of animal models, however, has allowed neuroscientists to harness the power of lesions by going beyond serendipity, and the function of countless brain areas has been elucidated through systematic studies of structure-function relationships through lesions[3,4].

To correctly assign function to a structure, however, lesion studies require precise quantification procedures, which is an area that has been lacking. The current gold standard for quantifying lesions is to section, mount, and image brains with a light microscope. The imaged slices are then matched to the closest sections on an atlas, and the approximate coordinates of the lesions across subjects are indirectly reported, often through the use of camera lucida images or example histological slices[3,4,5,6,7,8,9,10].

Beyond the imprecision of current lesion quantification procedures, these techniques are time-consuming and prone to failure. Small changes in brain stiffness, blade sharpness, and temperature can lead to botched, warped, or torn sections. Sections can also stain unevenly and be improperly imaged because of bubbles in the mounting medium. Importantly, upon sectioning, the three-dimensional context of the lesion's location in the brain is lost, making precise 3D reconstruction of the lesion in the brain challenging.

Another common application for lesions has been to determine the location of single and multiple electrode recordings in the brain. At the end of the final recording session, researchers induce small electrolytic lesions at the electrode tip and process the brain histologically as done in a conventional lesion experiment[11]. This technique suffers from the same drawbacks described above, with additional problems being that the electrolytic lesions are usually larger than the electrodes used to make them but are usually small enough that they are challenging to find histologically. When multiple electrodes are inserted, as in the case of a tetrode array, verification through electrolytic lesions is even more challenging. An alternative to electrolytic lesions is the use of a dye on the electrode to later verify histologically[12], but this technique suffers from the same drawbacks that come with conventional histology.

Here, we describe in-depth a recently described method[13] based on staining techniques in electron microscopy (EM) and X-ray computed tomography (micro-CT) that quantifies lesions and locates electrodes in small animal brains better than current methods. Micro-CT is an imaging technique in which X-rays are shot at a sample that is rotated 360° while a scintillator collects the X-rays not deflected by the sample. The result

is a high-resolution digital 3D reconstruction of the sample that can be visualized in any orientation and quantified precisely. Many academic institutions have micro-CT scanners, which are also available commercially.

Protocol

All care and experimental manipulation of animals were reviewed and approved by the Harvard Institutional Animal Care and Use Committee. The perfusion described here is specific for rats, but the procedure is applicable to any animals with smaller or similarly sized brains.

1. Perfusion

1. Prepare 1x phosphate-buffered saline (PBS). For a rat (age: 0.5–1.5 years old, weight: 250–600 g), 800–1,000 mL should be sufficient. Use 400 mL to perfuse the animal and an additional 400 mL to dilute the fixative.
2. Prepare the fixative consisting of 2% (w/v) paraformaldehyde (PFA) and 2.5% (w/v) glutaraldehyde (GA) in 1x PBS. For a rat, 400 mL is sufficient. Save 50 mL in a 50 mL conical tube for post-fixation of the brain after perfusion.
3. Anesthetize the rat with 4–5% isoflurane gas (at 0.8 L/min O_2 at 1.0 bar at 21 °C) for 15 min.
4. Inject a lethal dose of sodium pentobarbital intraperitoneally (180 mg/kg).
5. Test for reflex loss in the animal by conducting a toe-pinch reflex exam. Wait to begin the perfusion until the animal has lost its reflex response.
6. Follow the previously described intracardial perfusion and brain extraction protocol[14] with the following solutions: perfuse the animal with 400 mL of 1x PBS at 125 mm Hg to remove the blood. Once all blood has been removed and replaced with 1x PBS, begin perfusing with 400 mL of a solution of 2% PFA and 2.5% GA dissolved in 1x PBS at 125 mm Hg.
   NOTE: If the procedure is being conducted in an animal that is not a rat, the only important components of the perfusion procedure are the use of 1x PBS and 2% PFA, 2.5% GA in 1x PBS. The solution volumes and perfusion pressure may be adjusted according to the species.

2. Post-fixation

1. Place the extracted brain in 2% PFA, 2.5% GA in 1x PBS solution (same solution used to perfuse the animal previously). Ensure that the solution volume is at least 10x the volume of the brain. For rats, place the brain in a 50 mL conical tube with 50 mL of solution. Store the sample in post-fixation for 2–3 days, shaking lightly at 4 °C.
   NOTE: If the sample is in a 50 mL conical tube, placing it horizontally on an orbital shaker will ensure the best results.
2. After the sample has been post-fixed for long enough, wash the sample in double-distilled water (ddH_2O), de-ionized water (diH_2O), or ultrapure water (see **Table of Materials**) four times for the following durations: 1, 1, 1, and 15 min.
   NOTE: For this protocol, ddH_2O, diH_2O, or ultrapure water should be interchangeable. For simplicity, ddH_2O will be used to refer to purified water henceforth.

3. Staining

CAUTION: For this step, conduct all solution preparations under a hood while using gloves.

1. Prepare at least 10x the brain volume of staining solution. For rat brains, prepare 50 mL of 2% (w/v) osmium tetroxide (OsO_4) in ddH_2O by combining 25 mL of stock 4% OsO_4 solution and 25 mL of ddH_2O.
   CAUTION: Osmium tetroxide is volatile and may cause temporary blindness and respiratory problems if not handled appropriately. Discard all materials that contact the osmium tetroxide in an appropriate chemical hazard container within a secondary container.
2. Place the brain in a new 50 mL conical tube and add the OsO_4 solution. The brain should begin to turn brown as OsO_4 reacts with lipids in the tissue.
3. Close the tube and seal it thoroughly with paraffin film (see **Table of Materials**) to ensure that it does not leak during incubation.
   NOTE: The osmium is volatile and will react mildly with the plastic of the tube, so sealing the tube properly is very important. The tube may be wrapped with aluminum foil for added protection.
4. Store the sealed tube at 4 °C, shaking lightly on an orbital shaker at 50 rpm for 2 weeks. Place the tube horizontally to ensure the best mixing. Ensure that the sample is fully submerged in the solution while shaking.
   NOTE: If the osmium is not allowed to circulate continuously, it may not fully penetrate the sample, so horizontal placement on the shaker is very important.

4. Embedding

1. After the sample has been incubated in OsO_4 for 2 weeks, wash it with ddH_2O 5 times at room temperature (RT) for the following durations: 1, 1, 1, 15, and 60 min to remove all the unbound OsO_4 in the sample.
   NOTE: The multiple exchanges, including the last 60 min exchange, are necessary to allow all the osmium in the circulatory system to diffuse out.
2. Wash the sample with ddH_2O for 30 min at 4 °C.
   NOTE: Osmium may continue to diffuse out of the sample, but its quantity should be greatly reduced from the previous step.
3. Dehydrate the sample with ethanol to eventually infiltrate it with resin. To dehydrate, replace the ddH_2O with 10–20 mL of the following ethanol dilutions (for 30 min each at 4 °C): 20% (v/v) ethanol and 80% (v/v) ddH_2O; 50% (v/v) ethanol and 50% (v/v) ddH_2O; 70% (v/v) ethanol and 30% (v/v) ddH_2O; 90% (v/v) ethanol and 10% (v/v) ddH_2O; 100% ethanol.
4. Prepare the acetone/resin dilutions as follows.
   1. Prepare 100 mL of the resin for embedding (see **Table of Materials**) as per the manufacturer's instructions.

2. To make the 33% (v/v) resin-67% acetone solution, pour 15 mL of resin into a 50 mL conical tube and add 30 mL of 100% glass-distilled acetone.
3. To make the 50% (v/v) resin-50% acetone, pour 22.5 mL of resin into a 50 mL conical tube and add 22.5 mL of 100% glass-distilled acetone.
4. To make the 67% (v/v) resin-33% acetone solution, pour 30 mL of resin into a 50 mL conical tube and add 15 mL of 100% glass-distilled acetone.
5. Use the remaining 32.5 mL of resin as the first solution of 100% resin below.

5. Begin the resin infiltration process by moving the sample through 10-20 mL of the following acetone and acetone/resin dilutions: 100% acetone for 30 min at 4 °C; 100% acetone for 30 min at 4 °C; and 100% acetone for 30 min at room temperature (RT).
NOTE: The rest of the infiltration process will take place at RT.
6. Immerse the sample in 33% (v/v) resin 67% acetone for 3 h at RT, then 50% (v/v) resin-50% acetone for 3 h at RT, 67% (v/v) resin 33% acetone for 3 h at RT, and 100% resin for 12 h at RT.
7. Make a fresh 50 mL batch of resin following the instructions on the bottle. Transfer the sample to the container in which it will be cured (*e.g.*, the disposable molds described in **Table of Materials**). Infuse the sample with fresh 100% resin for 4 hours at RT.
NOTE: If fresh resin is not used, the resin made the previous day will begin to harden prematurely, and the sample will be hard to manipulate.
8. Degas the sample in a vacuum oven for 15 min at 45 °C.
NOTE: This step will help remove any trapped air bubbles within the sample, but it is non-essential and will not affect quality of the data.
9. Finally, cure the sample in an oven for 48 h at 60 °C.

5. micro-CT

1. Once the sample has been cured, peel off the disposable mold and scan it with the micro-CT machine.
NOTE: Depending on the machine used, the settings will be different. For the scanner used by the authors listed in the **Table of Materials**, the recommended settings are 130 kV, 135 µA with a 0.1 mm copper filter and a molybdenum source, a 1-second exposure, and an average of 4 frames per projection. However, experimenters should calibrate the scanner individually, as many factors will affect optimal settings during a particular session.
2. Once the scan is completed, reconstruct the sample with the recommended parameters for the experimenter's scanner/software combination on a computer with the scanner software.
3. Finally, visualize and analyze the reconstructed digital volume using the experimenter's software of choice (see **Table of Materials** for examples).

Representative Results

Traditionally, brains are sectioned and stained in order to quantify lesions and locate electrodes, but this method is error-prone, labor-intensive, and typically requires estimation of the results. By preparing whole brains for micro-CT imaging, the probability of damaging the samples is greatly reduced, features of interest may be analyzed in the context of the entire brain, and the method lends itself to parallel processing of many samples, considerably speeding up sample preparation.

The method involves four major steps: (1) staining a perfused brain with osmium tetroxide, (2) embedding the brain in resin, (3) imaging the brain with a micro-CT scanner, and (4) analyzing the resulting digital volume (**Figure 1**). In this article, only steps 1–3 are described, as step 4 (the analysis) will vary considerably depending on specific needs of the project.

Whereas in traditional sectioning in which one sectioning orientation must be chosen beforehand, the resulting digital volume from this method may be manipulated in three dimensions and virtually sliced in any orientation (**Figure 2a-2b**). The user may also scan a subsection of the sample at a higher resolution if desired, such as the olfactory bulb of a rat brain, where nerve fibers and individual glomeruli are visible (**Figure 2c**). The method is also broadly applicable to small animal brains. To verify this, a zebra finch brain was prepared using the same protocol used for the rat brains and resulted in a successful digital volume (**Figure 2e**). Scanning electron microscopy (SEM) of a sample prepared for micro-CT confirmed that the tissue was not damaged up to an order of magnitude in resolution beyond the micro-CT's resolution (**Figure 2d**). However, it should be noted that there was considerable ultrastructural damage, making this technique unsuitable for electron microscopy (EM).

The technique may be used to find surface lesions (**Figure 3**) and lesions deep within the brain (**Figure 4**). The technique also permits the locating of single tetrodes *in situ*, electrolytic lesions, electrode tracks of sufficient diameter, tetrode arrays *in situ,* and silicon probes *in situ* (**Figure 5**).

Unsuccessful preparations will comprise incomplete mineralization of the tissue, which may also occur if incorrect buffers are used (**Figure 6**). However, if only surface features are necessary, for example, then surface-only staining of the sample may be sufficient for the experimenter.

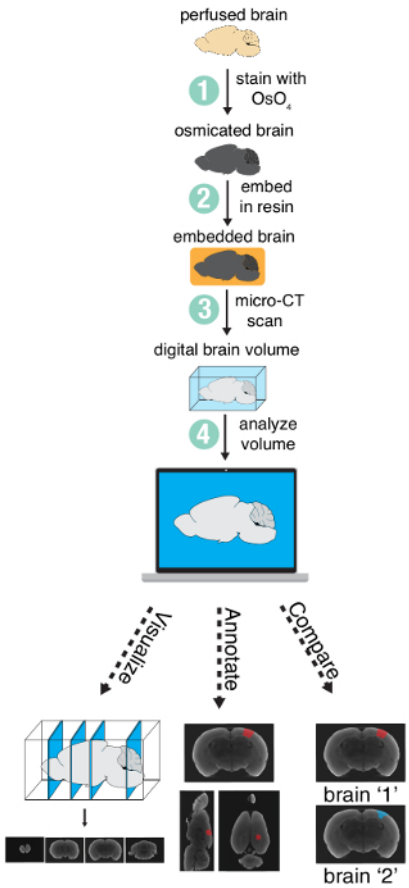

Figure 1: Method overview. Overview of the steps required to prepare and analyze a whole brain using micro-CT imaging. Figure used with permission from the authors[13]. Please click here to view a larger version of this figure.

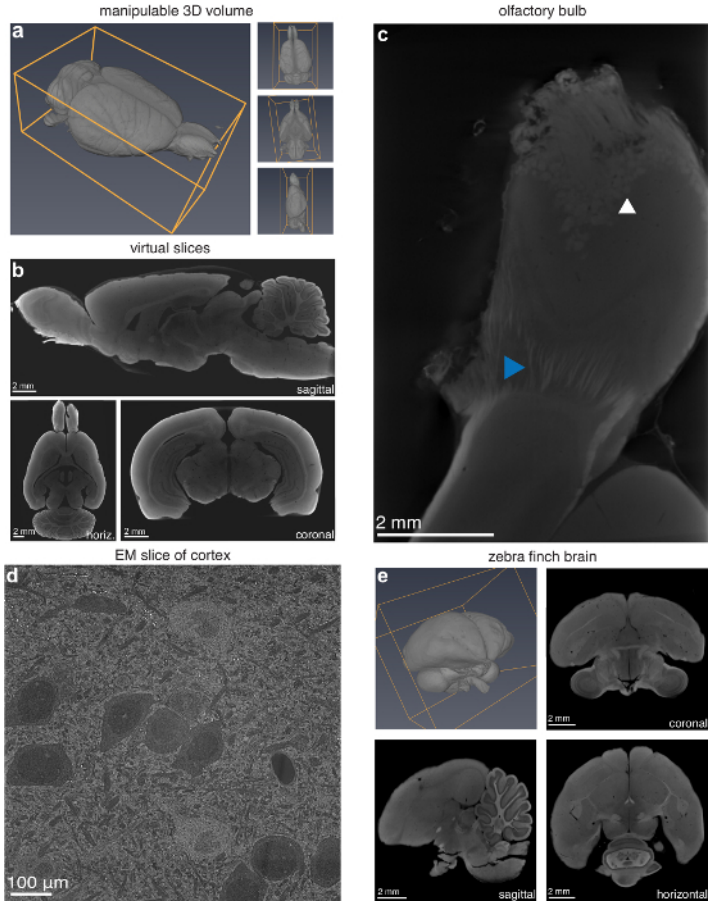

Figure 2: Capabilities of lesion characterization through micro-CT imaging. (**a**) Manipulatable 3D volume and (**b**) virtual slices (13.9 µm voxels) at arbitrary orientations from a micro-CT scan of a Long-Evans rat. (**c**) Olfactory bulb scanned at higher resolution (4.9 µm voxels) revealing glomeruli (white arrowhead) and individual nerve fibers (blue arrowhead). (**d**) Scanning electron microscope (SEM) image (10 nm/pixel) of the visual cortex of a rat brain prepared for micro-CT imaging. (**e**) Zebra finch (*Taeniopygia guttata*) brain prepared for micro-CT imaging; 3D volume and 2D slices (5.6 µm voxels) in the coronal, horizontal, and sagittal planes. Figure used with permission from the authors[13]. Please click here to view a larger version of this figure.

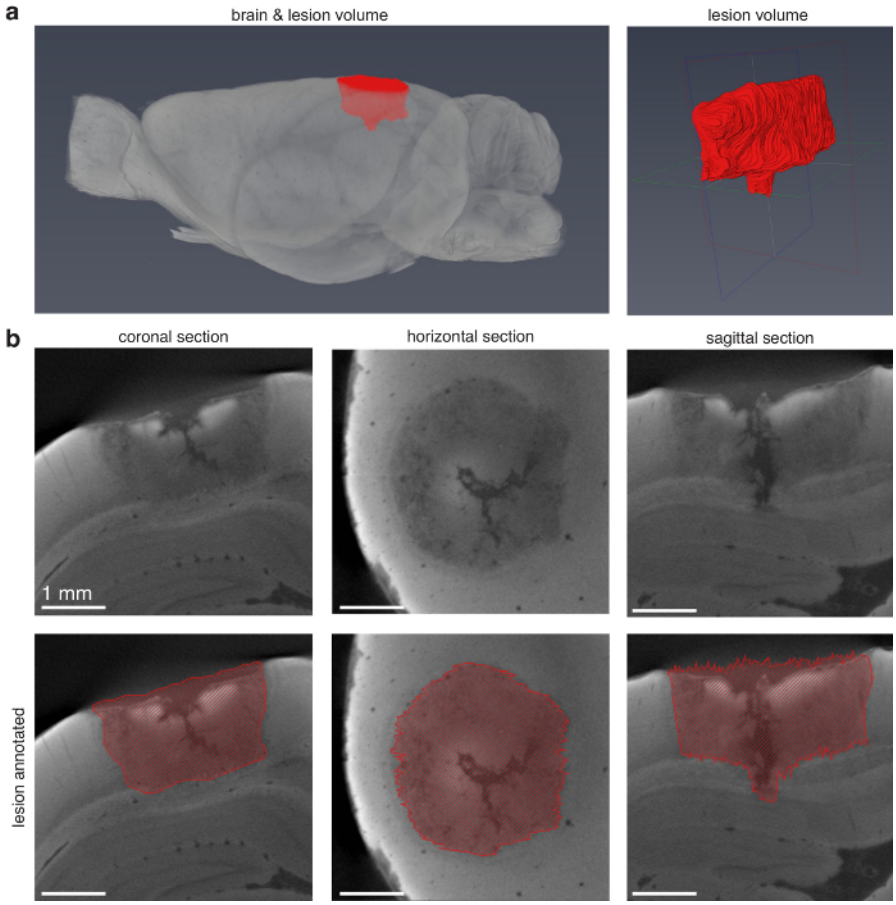

Figure 3: Visual cortex lesion characterization using micro-CT. (**a**) 3D visualization of a rat brain lesioned in the visual cortex with quinolinic acid. The left panel shows lesion volume in the context of the brain (brain made slightly transparent to allow visual access to the lesion). The right panel shows isolated lesion volume. (**b**) 2D slices of lesion in the coronal, horizontal, and sagittal planes (12.8 µm voxels). The top 3 panels show the unsegmented sections, and the bottom 3 panels show sections with overlaid lesion annotation. This lesion was manually annotated in the coronal orientation every 2 slices. The volume was then created through interpolation. Figure used with permission from the authors[13]. Please click here to view a larger version of this figure.

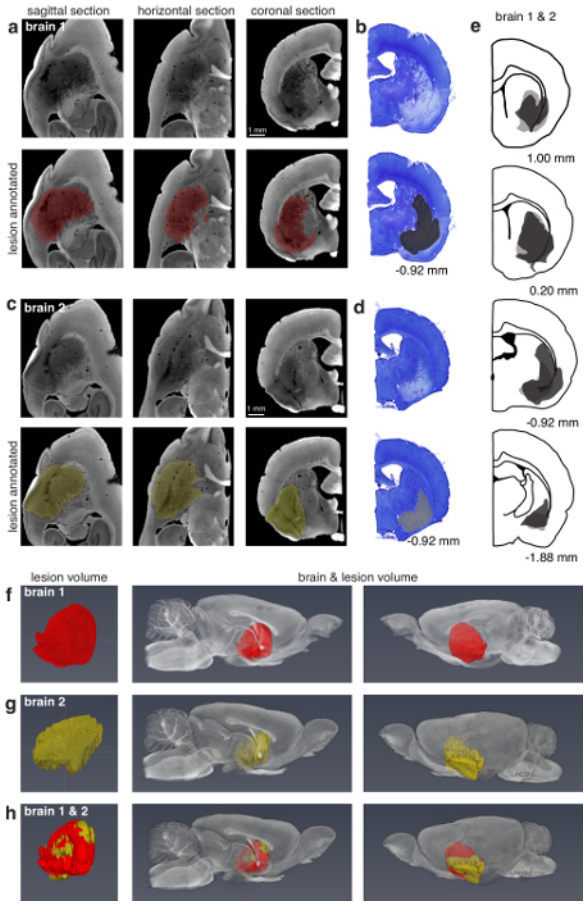

Figure 4: **Comparison of dorso-lateral striatum lesion characterization using micro-CT and histology.** (**a**) Sagittal, horizontal, and coronal views of the left half of "brain 1" processed for micro-CT imaging (13.5 µm voxels). The top 3 panels show unsegmented sections, and the bottom 3 panels show the annotated lesion on the same sections. The lesion was manually segmented in the sagittal plane every 2 sections and subsequently interpolated. (**b**) Closest matching coronal section of the right half of "brain 1" processed histologically for light microscopy. Panels (**c, d**) are similar to (a, b) but correspond to "brain 2". The brain 2 lesion was manually segmented in the coronal plane every 8 sections. (**e**) Lesion characterization of histology-treated right halves of brains 1 (dark grey) and 2 (light grey). The numbers in (b, d, e) underneath the panels correspond to positions relative to bregma. (**f**) Lesion characterization of the left half of brain 1 processed for micro-CT. The first panel shows the isolated lesion. The second and third panels show the lesion in context of the brain from two viewpoints. (**g**) Same as (f) but corresponding to brain 2. (**h**) An overlay of the lesions in (f, g) illustrating the capability for comparison of lesion characterization with digital brain volumes. The lesion in (f) was registered to the lesion in (g), and both are shown in the context of the left half of brain 2. Figure used with permission from the authors[13]. Please click here to view a larger version of this figure.

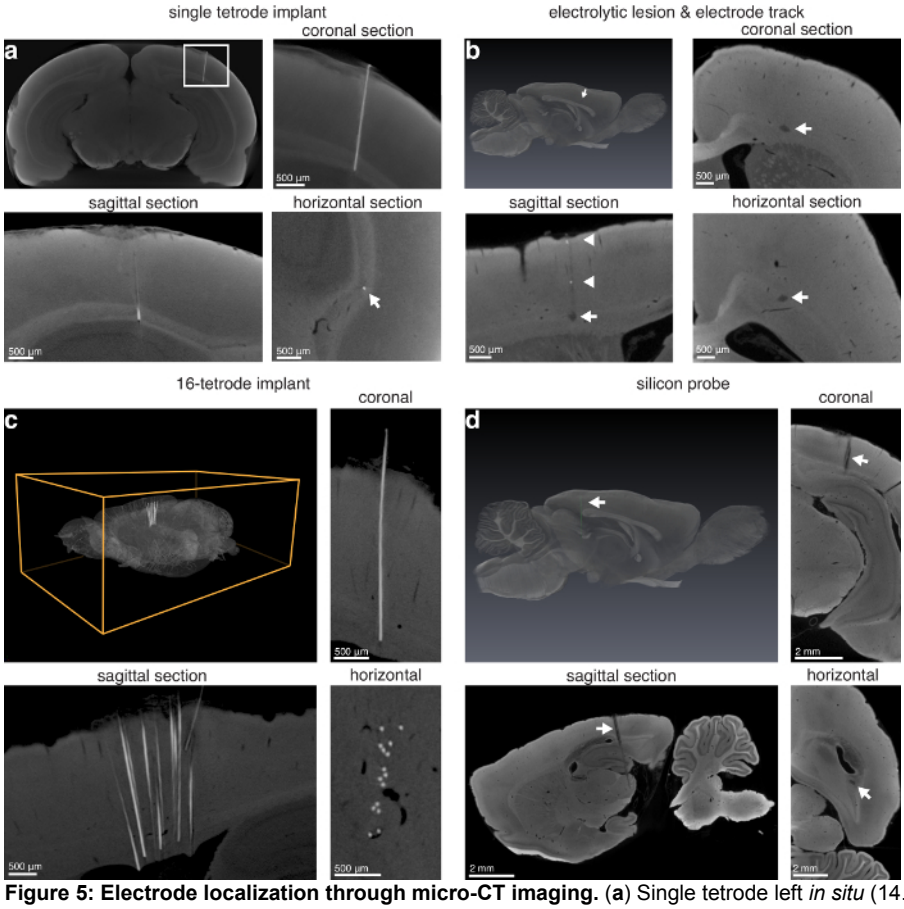

Figure 5: Electrode localization through micro-CT imaging. (**a**) Single tetrode left *in situ* (14.0 µm voxels). Top left panel: max-intensity projection of virtual coronal sections showing the location of a nichrome tetrode traveling through the visual cortex into the corpus callosum of a rat; top right: close-up of an image shown in the top left panel of (a) (white rectangle). Bottom left: sagittal; bottom right: horizontal views of the implanted electrode (white arrow indicates location of the tetrode). (**b**) Electrolytic lesion and electrode track in the anterior region of a rat brain (13.9 µm voxels). Top left: 3D rendering of a brain with the electrolytic lesion segmented out (white arrow indicating purple lesion); top right: coronal. Bottom left: sagittal; bottom right: horizontal sections indicating electrolytic lesion (white arrows) produced with a 75 µm diameter tungsten electrode. In addition, some metal deposited by the electrode upon retraction is visible along the track in the sagittal view (white arrowheads). (**c**) 16-tetrode implant left *in situ* in the anterior cortex of a rat brain. Top left: 3D rendering of a whole brain with a 16-tetrode array left implanted; top right: coronal. Bottom left: sagittal; bottom right: horizontal sections indicating a 16-tetrode implant (8.9 µm voxels). (**d**) Silicon probe (10 mm shank, 32 sites) left *in situ* traveling through the posterior cortex, hippocampus, and subcortical structures (13.9 µm voxels). Top left: 3D rendering of a whole brain with a segmented silicon probe (white arrow indicating green probe); top right: coronal. Bottom left: sagittal; bottom right: horizontal views of a silicon probe in the brain. Additionally, the reference site on the silicon probe is visible in the coronal and sagittal sections (tip of white arrows). Figure used with permission from the authors[13]. Please click here to view a larger version of this figure.

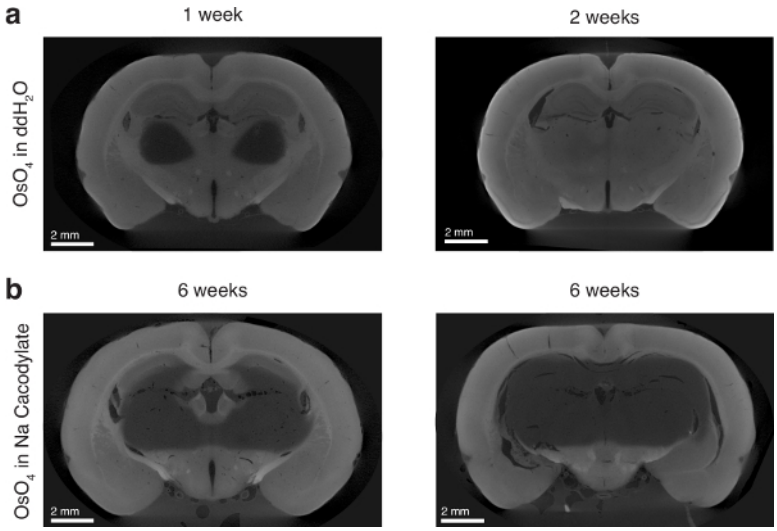

Figure 6: Effect of osmium tetroxide solvent on osmium penetration. (**a**) Left panel: rat brain incubated in osmium tetroxide in ddH_2O for 1 week. Right panel: rat brain incubated in osmium tetroxide in ddH_2O for 2 weeks. (**b**) Two rat brains incubated in osmium tetroxide in sodium cacodylate buffer for 6 weeks. Figure used with permission from the authors[13]. Please click here to view a larger version of this figure.

Discussion

The following are critical steps to the protocol: first, the use of a combination of PFA and GA to perfuse the animal and subsequently post-fix the brain was paramount to achieving consistent full osmium penetration of the tissue. Although we did not test this explicitly, a plausible explanation is that PFA fixation is reversible[15], whereas GA fixation is not reversible[16,17]. Because a two-week incubation in osmium tetroxide is required for full infiltration of the tissue, it is possible that the PFA in the interior of the brain diffuses out and the tissue degrades during the staining. The osmium thus cannot preserve the interior structures.

The use of aqueous osmium, as opposed to osmium dissolved in a buffer *(i.e.,* sodium cacodylate), was absolutely necessary to ensure full tissue penetration by the osmium. Even after a 6 week incubation, osmium dissolved in sodium cacodylate did not infiltrate the tissue completely and appeared to encounter a diffusion barrier (**Figure 6**). Osmium is extremely reactive to lipids and thought to bind those in cell membranes[18,19,20]. If the tissue is not sufficiently permeabilized, as might be the case with a gentle buffer like sodium cacodylate, it is possible that the cell membranes may saturate with osmium and sterically prevent more osmium from diffusing into the tissue. We hypothesize, however, that water as a solvent for the osmium acts as a light detergent and permeabilizes the tissue sufficiently to allow deep diffusion into the tissue.

If experimenters are preparing a smaller brain, such as that of a mouse, the incubation time in osmium can likely be reduced. Similarly, the incubation time needs to be increased in larger samples. This can be tested to determine the minimum time for consistent staining in a brain that is different in size than that of a rat. If experimenters encounter problems with full osmium infiltration, the likely problems are not using both PFA and GA during perfusion and post-fixation, not using water as the solvent for osmium (as discussed above), and insufficient agitation during osmium incubation. We found, for instance, that when incubating in 50 mL conical tubes, laying the tubes on their side (as opposed to vertically on a holder), filling them with stain, and placing them on an orbital shaker at 50 rpm for the entire incubation period ensured proper infiltration.

This method is limited in several ways. First, the preparation does not preserve ultrastructure very well, so it should not be used for electron microscopy. This method cannot be combined with any further histology or immunofluorescence. The resolution of the digital volume is determined by the size of the sample (smaller samples can be scanned at higher resolutions) and by the geometry of the scanner, if it relies on geometric magnification; however, subsections of the sample can be scanned at higher resolutions, if desired.

A new method combining electron microscopy-style tissue treatment with micro-CT imaging for quantifying lesions and localizing electrodes in small animal brains has been presented. This method is arguably less laborious, requires less expertise, and yields quantifiable results more easily than the current gold standard for sectioning and staining a brain. Previously, scientists have described a protocol for even osmium penetration in mouse brains that is meant to preserve ultrastructure for electron microscopy[21,22]. This protocol, however, is quite complex. In this study, the authors aimed to develop a much simpler method for micro-CT imaging rather than electron microscopy. There have been other studies applying micro-CT to imaging brains for various purposes. A previous investigation in rabbits and mice used micro-CT to find tumors and other abnormalities[23]. This investigation made use of proprietary MRI contrast agents, but the researchers did predict micro-CT's potential usefulness in lesion studies. Another study in mice aimed at finding gross morphological differences for a drug screen involved the staining of mouse brains with iodine in the skull, but the authors faced uneven tissue shrinkage and opted to embed the tissue in a hydrogel[24]. Other studies in mice have aimed to find cerebral cavernous malformations, a disorder of abnormally large and irregular capillaries, and have made use of osmium tetroxide and aqueous iodine as stains; however, these were performed in much smaller samples (detached mouse hindbrains) than described here[25,26,27]. Alternative methods for generating 3D brain volumes are μMRI[28] and high-resolution episcopic microscopy[31]. The resolution of μMRI is poorer (~25 μm voxels for similar samples[28]), and the technique is more expensive[23,30]. High-resolution episcopic microscopy also faces challenges: that it is a destructive technique, and a block-face apparatus allowing whole-brain sectioning would need to be produced. The work presented here also extends previous efforts to locate electrodes in the brain with X-rays[32,33,34] by capturing both the electrode and surrounding tissue. Furthermore, the technique allows for locating single electrodes, tetrode arrays, electrolytic lesions, electrode tracks, and silicon probes.

A valuable future direction would creation of an "average brain" atlas to which lesion studies could be co-registered to standardize lesion location and size quantification. This method may also be expanded to other model and non-model organisms, as exemplified by its immediate application to the zebra finch brain (**Figure 2**).

Disclosures

The authors have nothing to disclose.

Acknowledgements

The authors thank Greg Lin and Arthur McClelland for their expertise with the micro-CT machine, David Richmond and Hunter Elliott at the Image and Data Analysis Core (IDAC) at Harvard Medical School for their image processing advice, and William Liberti at Boston University for graciously providing a zebra finch brain. This work was performed in part at the Center for Nanoscale Systems (CNS), a member of the National Nanotechnology Coordinated Infrastructure Network (NNCI), which is supported by the National Science Foundation under NSF award no. 1541959. CNS is a part of Harvard University. This work was supported by the Richard and Susan Smith Family Foundation and IARPA (contract #D16PC00002). S.B.E.W. was supported by fellowships from the Human Frontier Science Program (HFSP; LT000514/2014) and the European Molecular Biology Organization (EMBO; ALTF1561-2013). G.G. was supported by the National Science Foundation (NSF) Graduate Research Fellowship Program (GRFP).

References

1. Scoville, W., Milner, B. Loss of recent memory after bilateral hippocampal lesions. *Journal of Neuropsychiatry and Clinical Neuroscience.* **12**, 103-13(2000).
2. Damasio, H., Grabowski, T., Frank, R., Galaburda, A.M., Damasio, A.R. The return of Phineas Gage: clues about the brain from the skull of a famous patient. *Science*. **264** (5162), 1102-1105 (1994).
3. Kawai, R., *et al.* Motor cortex is required for learning but not for executing a motor skill. *Neuron.* **86**, 800-812 (2015).
4. Otchy, T., *et al.* Acute off-target effects of neural circuit manipulations. *Nature.* **528**, 358-363 (2015).
5. Wright, N., Vann, S., Aggleton, J., Nelson, A. A critical role for the anterior thalamus in directing attention to task-relevant stimuli. *Journal of Neuroscience.* **35**, 5480-5488 (2015).
6. Kapgal, V., Prem, N., Hegde, P., Laxmi, T., Kutty, B. Long term exposure to combination paradigm of environmental enrichment, physical exercise and diet reverses the spatial memory deficits and restores hippocampal neurogenesis in ventral subicular lesioned rats. *Neurobiology of Learning and Memory.* **130**, 61-70 (2016).
7. Hosseini, N., Alaei, H., Reisi, P., Radahmadi, M. The effects of NBM- lesion on synaptic plasticity in rats. *Brain Research.* **1655**, 122-127 (2017).
8. Palagina, G., Meyer, J., Smirnakis, S. Complex visual motion representation in mouse area V1. *Journal of Neuroscience.* **37**, 164-183 (2017).
9. Ranjbar, H., Radahmadi, M., Reisi, P., Alaei, H. Effects of electrical lesion of basolateral amygdala nucleus on rat anxiety-like behavior under acute, sub-chronic, and chronic stresses. *Clinical and Experimental Pharmacology and Physiology.* (2017).
10. Wood, R., *et al.* The honeycomb maze provides a novel test to study hippocampal-dependent spatial navigation. *Nature.* (2018).
11. Vermaercke, B., *et al.*Functional specialization in rat occipital and temporal visual cortex. *Journal of Neurophysiology.* **112**, 1963-1983 (2014).
12. Jun, J.J., et al. Fully integrated silicon probes for high-density recording of neural activity. *Nature.* **551**, 232-236 (2017).
13. Masís, J., *et al.* micro-CT-based method for quantitative brain lesion characterization and electrode localization. *Scientific Reports.* **8**, 5184 (2018).
14. Gage, G., Kipke, D.R., Shain, W. Whole Animal Perfusion Fixation for Rodents. *Journal of Visualized Experiments.* **65**, 3564 (2012).
15. Helander, K. Kinetic studies of formaldehyde binding in tissue. *Biotechnic & Histochemistry.* (1994).
16. Paljärvi, L., Garcia, J., Kalimo, H. The efficiency of aldehyde fixation for electron microscopy: stabilization of rat brain tissue to withstand osmotic stress. *Histochemical Journal.* (1979).
17. Okuda, K., Urabe, I., Yamada, Y., Okada, H. Reaction of glutaraldehyde with amino and thiol compounds. *Journal of Fermentation and Bioengineering.* **71,** (1991).
18. Bahr, G. Osmium tetroxide and ruthenium tetroxide and their reactions with biologically important substances: electron stains III. *Experimental Cell Research.* (1954).
19. Khan, A. A., Riemersma, J. C., Booij, H. L. The reactions of osmium tetroxide with lipids and other compounds. *Journal of Histochemistry & Cytochemistry.* **9**, 560-3 (1961).
20. Riemersma, J. Osmium tetroxide fixation of lipids for electron microscopy a possible reaction mechanism. *Biochimica et Biophysica Acta.* **152,** (1968).
21. Mikula, S., Binding, J., Denk, W. Staining and embedding the whole mouse brain for electron microscopy. *Nature Methods.* **9**, 1198-1201 (2012).
22. Mikula, S., Denk, W. High-resolution whole-brain staining for electron microscopic circuit reconstruction. *Nature Methods.* **12**, 541-546 (2015).
23. Crespigny, A., *et al.* 3D micro-CT imaging of the postmortem brain. *Journal of Neuroscience Methods.* **171**, 207-213 (2008).
24. Anderson, R., Maga, A. A novel procedure for rapid imaging of adult mouse brains with MicroCT using Iodine-Based contrast. *PLoS One.* **10**, e0142974 (2015).
25. Zhou, Z., *et al.* Cerebral cavernous malformations arise from endothelial gain of MEKK3-KLF2/4 signalling. *Nature.* **532**, 122-126 (2016).
26. Choi, J., *et al.* Micro-CT imaging reveals mekk3 heterozygosity prevents cerebral cavernous malformations in Ccm2-Deficient mice. *PloS One.* **11**, e0160833 (2016).
27. Choi, J., Yang, X., Foley, M., Wang, X., Zheng, X. Induction and Micro-CT imaging of cerebral cavernous malformations in mouse model. *Journal of Visualized Experiments.* (2017).
28. Benveniste, H., Kim, K., Zhang, L., Johnson, G. Magnetic resonance microscopy of the C57BL mouse brain. *Neuroimage.* **11**, 601-611 (2000).

29. Weninger, W. J., *et al.* High-resolution episcopic microscopy: a rapid technique for high detailed 3D analysis of gene activity in the context of tissue architecture and morphology. *Anat Embryol.* **211**, 213-21 (2006).
30. Schneider, J. E., *et al.* High-resolution, high-throughput magnetic paragraph sign resonance imaging of mouse embryonic paragraph sign anatomy using a fast gradient-echo sequence. *MAGMA.* **16**, 43-51 (2003).
31. Sharpe, J. Optical projection tomography. *Annual Review of Biomedical Engineering.* **6**, 209-28 (2004).
32. Cox, D. D., Papanastassiou, A., Oreper, D., Andken, B., James, D. High-Resolution Three-Dimensional microelectrode brain mapping using stereo microfocal x-ray imaging. *Journal of Neurophysiology.* **100**, 2966-2976 (2008).
33. Borg, J. S., *et al.* Localization of metal electrodes in the intact rat brain using registration of 3D microcomputed tomography images to a magnetic resonance histology atlas. *eNeuro.* **2**, (2015).
34. Fu, T.-M., *et al.* Stable long-term chronic brain mapping at the single-neuron level. *Nature Methods.* **13**, 875-882 (2016).

